Acta Cryst. (1977). B33, 1765–1773

The Structure of Tetraiodoethylene at 4 K

BY B. C. HAYWOOD

Materials Physics Division, Atomic Energy Research Establishment, Harwell, Oxfordshire England

AND R. SHIRLEY

Department of Chemical Physics, University of Surrey, Guildford, Surrey, England

(*Received* 16 *September* 1976; *accepted* 15 *November* 1976)

The crystal and molecular structure of tetraiodoethylene (C_2I_4) at 4 K has been determined by neutron powder diffraction with Rietveld's profile-refinement method. Three independent data sets at different wavelengths were collected and used in the calculations. The measurements were sufficiently accurate to locate the C atoms in the molecules, and to show that the C=C bonds in both molecules are fully ordered and aligned approximately parallel to **a***. The dimensions of the unit cell at 4 K and several interatomic distances are reported. The estimated standard deviations derived by this method are discussed and a normalization and weighting scheme for combining results from multiple power-data sets is suggested.

Introduction

Tetraiodoethylene is a crystalline solid whose structure at room temperature was reported by Khotsyanova, Kitaigorodsky & Struchkov (1952, 1953), and Kitaigorodsky, Khotsyanova & Struchkov (1953) in a three-dimensional single-crystal X-ray structure analysis. The monoclinic $P2_1/c$ cell was found to contain two independent molecules (*A* and *B*) in the asymmetric unit, with centres at two of the non-equivalent inversion centres of this space group.

An important aspect of the structure left undecided was the orientations of the C=C bonds in the two molecules. The difficulty in determining these arises from the fact that the molecule is planar and the I atoms lie very nearly at the vertices of a square. Thus, for each molecule, determination of the I positions does not decide along which of two directions the C=C bond lies. The C atoms themselves could not be located in the final Fourier syntheses. Their scattering factor is only about one tenth that of I for this radiation.

The structure determination was reviewed by Kitaigorodsky (1961), who pointed out that the intermolecular packing was affected very little by the C positions. He proposed that the two orientations were adopted statistically with equal probability, and that this disorder was the cause of the inability to detect the C atoms.

A further single-crystal study by Kipps (1973) gave improved cell constants but again did not succeed in locating the C atoms. Because only two-dimensional *h*0*l* intensity data were used, Kipps could not determine the I *y* coordinates. Hence, the best available room-temperature X-ray data are obtained by combining Kipps's cell with the three-dimensional coordinates of Kitaigorodsky *et al.* (1953). This is shown in Table 1 and incorporates several corrections to the original calculations.

The intramolecular geometry of C_2I_4 is well established from its molecular complexes with 1,4-diselenane (Dahl & Hassel, 1965) and pyrazine (Dahl & Hassel, 1968). More precise values were obtained from the vapour-phase electron diffraction study of Strand (1967), whose values are given in Table 2. Thus the main feature of the C_2I_4 crystal structure as yet undetermined is the nature of the C=C bond orientations. For each molecule, C=C could be either (1) ordered and aligned approximately parallel to **a***; (2) ordered and approximately parallel to **c**; or (3) occupying both these orientations statistically, the simplest distribution being with 0·5 occupancy of each orientation. Because the *A* and *B* molecules are not related by symmetry, they could take up these orientations independently, giving a total of nine possible configurations for the structure as a whole.

A spectroscopic study has been made by Thackeray, Shirley, Oralratmanee, Kipps & Stace (1974) to try to determine the C=C orientations by single-crystal Raman and polarized IR techniques. Their results indicated that probably more of the C=C bonds are oriented along the **a*** direction. However, the methods used, and the presence of twinning, did not allow the relative proportions of the two orientations to be estimated with much accuracy, nor distinguish between the orientations of the *A* and *B* molecules.

Because of the difficulty of growing sufficiently large untwinned crystals, a single-crystal neutron structure determination has not yet been undertaken. In the past,

Table 1. *Structural geometry*

	X-ray single-crystal[1] (room temperature)	Neutron set 1 1·538 Å 25 parameters	Neutron set 2 2·407 Å 30 parameters	Neutron set 3 2·434 Å 30 parameters	Neutron weighted mean[3] set 1,2,3 2:5:3
Intramolecular					
Bonds (Å)					
C(1)=C(1)′	(1·34)	—	1·229 (17)	1·254 (26)	1·238 (29)
C(3)=C(3)′		—	1·372 (16)	1·319 (25)	1·352 (26)
I(1)—C(1)	(2·10)	—	2·185 (22)	2·214 (31)	2·196 (35)
I(2)—C(1)		—	2·073 (17)	2·117 (26)	2·090 (29)
I(3)—C(3)		—	2·093 (19)	2·127 (28)	2·106 (32)
I(4)—C(3)		—	2·088 (22)	2·024 (33)	2·064 (36)
Angles (°)					
I(1)—C(1)—I(2)	—	—	111·8 (8)	112·6 (12)	112·1 (14)
I(3)—C(3)—I(4)	—	—	113·6 (8)	113·1 (11)	113·4 (12)
I(1)—C(1)—C(1)′	—	—	118·8 (11)	113·8 (15)	116·9 (18)
I(2)—C(1)—C(1)′	—	—	129·3 (13)	133·2 (19)	130·8 (21)
I(3)—C(3)—C(3)′	—	—	122·4 (12)	120·3 (18)	121·6 (19)
I(4)—C(3)—C(3)′	—	—	123·9 (11)	126·6 (17)	124·9 (18)
Contacts (Å)					
I(1)···I(2)	3·57 (1)	3·423 (27)	3·527 (20)	3·605 (29)	3·529 (30)
I(3)···I(4)	3·62 (2)	3·506 (32)	3·498 (23)	3·464 (32)	3·489 (35)
I(1)···I(2)′	3·61 (2)	3·641 (29)	3·609 (23)	3·636 (35)	3·624 (35)
I(3)···I(4)′	3·61 (2)	3·718 (28)	3·660 (19)	3·605 (28)	4·057 (18)
Intermolecular					
Contacts (Å)					
I(1)···I(2)[15][2]	3·77 (2)	3·786 (30)	3·720 (23)	3·641 (34)	3·709 (35)
I(1)···I(1)′[10]	4·14 (1)	4·223 (23)	4·057 (18)	4·119 (25)	4·109 (26)
I(1)···I(4)	4·05 (1)	3·899 (27)	4·074 (19)	4·093 (29)	4·045 (30)
I(2)···I(4)[1]	3·84 (2)	3·687 (34)	3·761 (24)	3·881 (37)	3·782 (38)
I(2)···I(3)[14]	3·95 (1)	4·069 (26)	3·935 (20)	3·928 (30)	3·960 (30)
I(3)···I(4)[15]	3·87 (1)	3·959 (27)	3·862 (20)	3·903 (28)	3·893 (30)
I(3)···I(3)′[8]	4·17 (2)	4·187 (32)	4·215 (24)	4·215 (34)	4·209 (36)
Interplanar angles (°)					
Molecule *A*: (010)	−25·4	−24·5	−24·5	−23·7	−24·3
Molecule *B*: (010)	26·5	27·5	27·1	29·0	27·8
A:*B*	51·6	52·0	51·6	52·6	52·0

Notes: (1) Combination of cell from Kipps (1973) with coordinates from Kitaigorodsky *et al.* (1953). (2) Numbers in square brackets refer to X-RAY 72 *BONDLA* program symmetry operations by which the contacting atom is generated (see Fig. 4). (3) E.s.d.'s derived from individual e.s.d.'s, normalized as described in the text.

Table 2. *Mean intramolecular geometry*

	Electron diffraction[1] (vapour)	Neutron diffraction[2] (powder, 4 K)
Bonds (Å)		
C=C	1·363 (15)	1·295 (20)
I–C	2·106 (5)	2·114 (16)
Angles (°)		
ICI	114·2 (5)	112·8 (9)
ICC	122·9 (3)	123·6 (10)
Contacts (Å)		
I(1)···I(2)	3·536 (5)	3·509 (23)
I(1)···I(2′)	3·652 (5)	3·640 (23)

Notes: (1) Strand (1967). (2) Weighted mean values from Table 1, averaged over chemically equivalent parameters (e.s.d.'s derived from individual e.s.d.'s, normalized as described in the text).

a neutron powder diffraction study of a material with such low symmetry would not have been practicable owing to the difficulty of analysing the great number of overlapping lines that are produced. Recently, however, a method has been devised (Rietveld, 1969*b*) by which a least-squares fit is computed to the experimentally measured angular distribution of scattered neutrons. This fit of the scattering profile is adjusted iteratively by changing the variables to be refined, which can include the cell constants and the parameters of the atoms in the unit cell.

Three short runs were made at 4 K on a neutron powder diffractometer, and from these data the refined positions and site occupancies of the C atoms in the tetraiodoethylene unit cell were found to confirm the predictions of Thackeray *et al.* (1974).

Experimental details

The neutron diffraction measurements were carried out on the PANDA instrument at the PLUTO reactor at Harwell. This neutron diffractometer is a conventional two-axis machine with a useful incident neutron flux in the range 0·9 to 2·5 Å. In the present series of experiments the monochromator used was of pressed germanium with mosaic around 8′ f.w.h.m. and the Soller-slit collimation between source and monochromator, monochromator and specimen, and specimen and counter was 15′, 60′ and 15′ respectively.

The intensity of scattered neutrons was expected to be quite small because of the low symmetry of the crystalline structure of the lattice and thus the first run was carried out with the incident neutron wavelength at a nominal value of 1·56 Å close to the maximum of the neutron source distribution. This wavelength was obtained from the germanium (511) plane at a take-off angle of 91·5°.

In addition to this, three detectors were mounted separately in the counter shield spaced 5·00 ± 0·02° apart in the horizontal (2θ) plane so as to maximize the detected count rate. As a further measure to increase the number of neutrons detected, the specimen was made as large as possible, being packed in a vanadium tube 12 mm diameter and 50 mm high, and cooled to 4 K to reduce the temperature factor.

The first run was carried out over 24 h and produced a scattered neutron distribution extending from 10 to 110° with a sufficient count/background ratio to enable preliminary analysis to be carried out. The quality of the data can be judged from Fig. 1 in which the summed counts of the three detectors are plotted as a function of counter take-off angle, 2θ, over an angular range which includes the most intense peak, $\bar{1}\bar{1}1$ centred at $2\theta = 22{\cdot}2°$.

It was found to be easily possible to fit these data by the refinement program described above but, although there were strong indications that the structure was at least partially ordered, the quality of fit did not allow a firm estimate of the degree of ordering to be determined.

Following the successful fitting of the first set of data a second run was carried out with the purpose of improving the data to the point where the degree of ordering in the crystal could be definitely established. One of the difficulties in the fitting procedure for the first set of data was caused by the very large number of diffraction lines encountered in the range 10 to 110° in 2θ. It was estimated that increasing the wavelength to 2·5 Å would reduce this number from *ca* 900 to *ca* 300 with a consequent improvement in the resolution.

Another advantage in using a longer incident neutron wavelength is that it permits an improved determination of the background count rate to be made. The background in neutron diffraction experiments comes almost entirely from neutrons scattered incoherently by the specimen. Great difficulty was experienced in determining its level in this series of experiments because of the almost continuous distribution in the diffraction pattern over most of the angular range. The use of a longer incident neutron wavelength produces increased spacing of the diffraction peaks and allows spaces to occur in this continuous distribution through which the background can be determined. The loss in neutron flux involved in going to a longer wavelength would be partially compensated by the increase in the scattering cross-section. A very convenient wavelength lies in the region of 2·4 Å because it is possible to use a pyrolytic graphite filter in the beam incident on the specimen, effectively eliminating all $\lambda/3$ contamination.

The second run was thus carried out with an incident neutron beam of *ca* 2·4 Å obtained from the Ge (311) plane at a take-off angle of 91°. The beam was passed

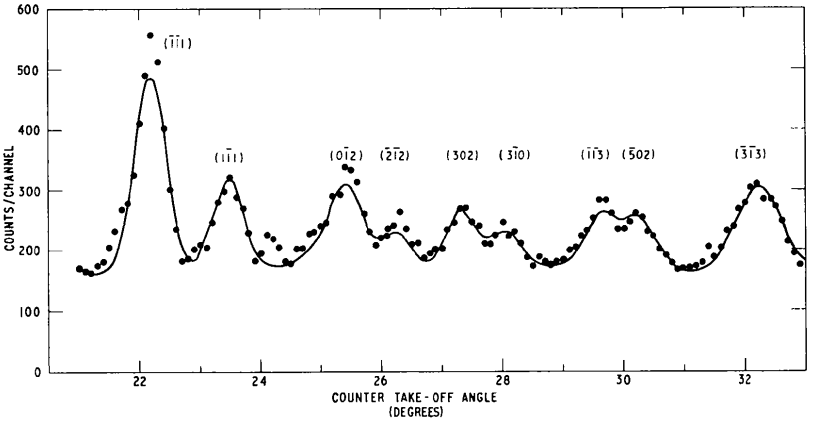

Fig. 1. Data from set 1 taken with $\lambda = 1{\cdot}538$ Å. The curve was produced by the 25-parameter fit with $R_I = 10{\cdot}95$.

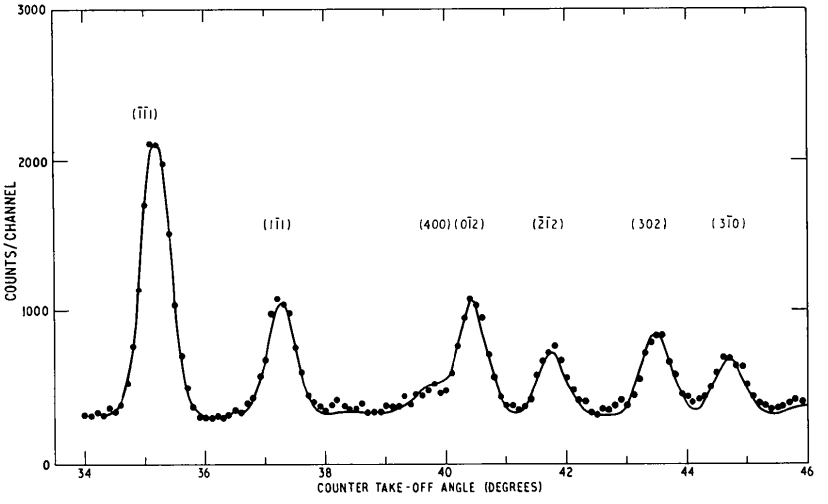

Fig. 2. Data from set 2 taken with $\lambda = 2{\cdot}407$ Å. The curve was produced by the 30-parameter fit with $R_I = 0{\cdot}30$.

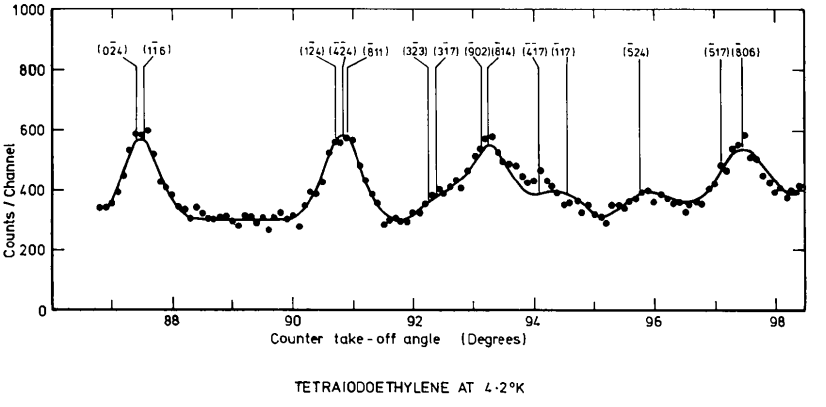

Fig. 3. Data from set 2 taken as for Fig. 2.

through a pyrolitic graphite filter, 30 mm thick, before striking the specimen. A check with a powdered Ni specimen failed to find any trace of the 111, 200, or 220 lines from any $\lambda/3$ component of this beam. Two runs were made, each of around 30 h duration with only a single neutron detector, and after initial examination were summed channel by channel. The resulting data were considerably better than those from the first run and enabled a much improved value of the ordering parameter for this crystal structure to be obtained. Some of the data are shown in Figs. 2 and 3. Fig. 2 covers the same peaks as were displayed in Fig. 1 and Fig. 3 shows part of the continuous distribution of overlapping peaks found at the higher angles.

Results

Data from the first run with neutrons of 1·56 Å nominal extended from a counter angle of 10 up to 110°. A representative section of these data is shown in Fig. 1, and the difficulties in determining the background count rate can be seen as the continuous distribution of overlapping lines extends unbroken from this graph up to the high-angle end of the data.

Determination of the exact value of the background level is more important in the present experiment than is usually the case, because of the low intensity of the diffracted peaks. It is known from previous experiments that the background of the PANDA machine under similar experimental conditions is not very dependent on counter angle and as a first trial a mean value of 163 counts/channel was assumed, taken from the spaces between the peaks at low angle.

The initial atomic parameters were taken from Kitaigorodsky (1961), with the population on each of the C positions set at 0·5. Half-width parameters were set so that calculated peaks would be wider than the measured peaks to ensure that a sufficiently wide range of angle would be searched by the program at each

peak. Cell parameters were those of Kipps (1973), but it was assumed that these would be only approximate as they referred to a room-temperature sample.

Details of the program have been given by Rietveld (1969*a*), the version used being that of Hewat (1973).

An important difference between this method and the more usual fitting procedure for powder diffraction data is that the latter minimizes the sum of the squares of the differences between observed (I_o) and calculated (I_c) peak areas, whereas the Rietveld method does so for the differences between observed (y_o) and calculated (y_c) counts in individual channels of the step scan. Thus the more directly relevant residual is $R_y = \Sigma|y_o - k^{-1} \times y_c|/\Sigma y_o$, where k is the scale factor of the observed data. A residual R_I comparable with that for the more conventional area method can be obtained by $R_I = \Sigma|I_o - k^{-1}I_c|/\Sigma I_o$, where $I_o(= F_o^2)$ has been obtained for each peak by apportioning every channel count y_o in proportion to the contribution of y_c for that reflexion and integrating over all relevant channels with due allowance for the Lorentz factor. The value obtained for R_I is approximately twice that of the conventional R, based on $|F|$, used in single-crystal studies. However, the integration process tends to smooth discrepancies, and R_I probably underestimates the true intensity residual. An 'expected' value of R_y is also printed by the program, based on counting statistics and the number of variable parameters employed. Residuals for each refinement are given in Table 3.

In using the program it is essential that the initial data are approximately correct if convergence is to be achieved. Analysis of the 1·56 Å nominal data was

Table 3. *Experimental measurements*

Data set			1	2		3
Wavelength (Å)						
nominal			1·562	2·44		—
calibrated			1·538 (1)	2·407 (2)		2·434 (2)
2θ range (°)			10–110	10–114		18–99
Duration (h)			24	60		20
Parameters refined			25	38	30	30
Residuals (%)						
Ry			22·00	15·84	15·79	20·53
Ry 'expected'			28·07	11·83	11·89	13·55
R_I			10·95	9·69	9·30	13·45
		Initial value				
Cell	a (Å)	15·027	14·931 (5)	14·932 (3)	14·932 (3)	14·928 (3)
	b (Å)	4·372	4·2712 (13)	4·2711 (9)	4·2710 (9)	4·2715 (7)
	c (Å)	12·866	12·684 (4)	12·684 (2)	12·684 (2)	12·686 (2)
	β°	109·32	108·36 (3)	108·34 (1)	108·34 (1)	108·35 (1)
I(1)	x	0·087	0·0959 (13)	0·0886 (11)	0·0885 (10)	0·0908 (16)
	y	0·267	0·2859 (40)	0·2715 (37)	0·2754 (35)	0·2800 (42)
	z	−0·119	−0·1189 (14)	−0·1246 (11)	−0·1139 (10)	−0·1216 (15)
I(2)	x	0·156	0·1512 (14)	0·1554 (12)	0·1557 (11)	0·1577 (18)
	y	0·585	0·6061 (39)	0·5960 (34)	0·5940 (30)	0·5932 (39)
	z	0·151	0·1412 (17)	0·1473 (15)	0·1463 (13)	0·1563 (19)
I(3)	x	0·411	0·4105 (14)	0·4086 (12)	0·4069 (10)	0·4085 (15)
	y	0·227	0·2265 (39)	0·2318 (41)	0·2296 (36)	0·2442 (49)
	z	−0·187	−0·1824 (17)	−0·1858 (15)	−0·1860 (12)	−0·1836 (16)
I(4)	x	0·342	0·3351 (16)	0·3441 (11)	0·3433 (10)	0·3467 (16)
	y	−0·126	−0·1368 (46)	−0·1336 (33)	−0·1326 (31)	−0·1371 (41)
	z	0·029	0·0228 (15)	0·0286 (12)	0·0274 (11)	0·0245 (16)
C(1)	x	0·045	(0·045)	0·0425 (10)	0·0424 (8)	0·0440 (13)
	y	0·474	(0·474)	0·4799 (38)	0·4789 (33)	0·4943 (46)
	z	0·006	(0·006)	0·0092 (13)	0·0084 (11)	0·0112 (16)
C(3)	x	0·455	(0·455)	0·4536 (9)	0·4531 (8)	0·4545 (13)
	y	0·018	(0·018)	0·0134 (33)	0·0125 (31)	0·0178 (47)
	z	−0·029	(−0·029)	−0·0299 (12)	−0·0302 (11)	−0·0263 (17)
Site population						
	C(1)	0·5	0·72 (3)	0·946 (17)	(1·0)	(1·0)
	C(2)	0·5	0·28 (3)	0·054 (17)	—	—
	C(3)	0·5	0·88 (3)	0·994 (16)	(1·0)	(1·0)
	C(4)	0·5	0·12 (3)	0·006 (16)	—	—

therefore carried out in many steps, increasing the number of parameters varied until there was no significant improvement in the fit. The first five-parameter refinement varied only the scale factor and the four cell parameters of the monoclinic lattice. It was immediately apparent that the cell had become distorted at the lower temperature and that the new parameters (uncalibrated) were $a = 15{\cdot}168\,(4)$, $b = 4{\cdot}338\,(1)$, $c = 12{\cdot}883\,(4)$ Å and $\beta = 108{\cdot}36\,(3)°$. Successive refinements and calibration correction (see below) led to the 25 parameters listed in Table 3, for which $R_I = 11{\cdot}0\%$. Increasing the number of refined parameters to include the C positions did not improve this fit significantly and it was concluded that the limit of this data set had probably been reached.

Table 3 shows that the population of the C atoms, which had been varied subject to the constraint that the total on each of the two competing pairs of sites was unity, was heavily weighted towards the C(1) and C(3) sites. These sites lie along the **a*** axis and thus tend to confirm the results of Thackeray *et al.* (1974). The quality of fit can be assessed from the curves drawn in Fig. 1. This indicates that while there may be some slight discrepancies, in general the predicted line passes through the measured points to the accuracy of measurement.

The second experiment, performed with incident neutrons of 2·44 Å nominal, produced data of a much better quality than the first. There was also less difficulty in the determination of the background level because of the greater spacing of the diffracted lines. The same refinement procedure was adopted for these data as for the previous case and it was found possible to refine the C positions as well as their population. The final value of the intensity residual R_I was 9·7% (conventional $R \simeq 4{\cdot}8\%$).

In view of the overwhelming preponderance of occupied C(1) and C(3) sites, the C(2) and C(4) sites were removed from the analysis leaving 30 parameters, and it was found that R_I dropped slightly to 9·3%. A measure of the degree of fit can be obtained from the graphs shown in Figs. 2 and 3 which show the final 30-parameter fit to the data at two points on the diffraction pattern.

In some of the early fits to these data, it was found that a negative isotropic temperature factor was produced by the program, *i.e.* the amplitude of motion of the atom was imaginary. In those cases it was found that a small increase in the background level at high angles, usually well within the estimated uncertainties, was sufficient to increase the temperature factor to a positive value. This also indicated that the values of the isotropic temperature factors were not meaningful, which is confirmed by the lack of success of an attempt to improve the degree of fit by including anisotropic I temperature factors in the refinement. This led in every case to negative diagonal terms in the B_{ij} matrix, despite attempts to rectify the situation by making reasonable increases in the estimated background at high angles.

Wavelength calibration

After completing refinement of data sets 1 and 2, a systematic error in the cell constants become apparent. The cell sides a, b and c for set 1 were greater than those for set 2 by 0·19, 0·20 and 0·20% respectively (*i.e.* +6 standard deviations), whereas the cell angle β, which has only a slight dependence on the wavelength used, agreed to 0·01°. In neither case did the values exhibit the marked contraction that might have been expected by comparison with the room-temperature cell. Clearly the effective neutron wavelength had been determined insufficiently accurately in one or both of the runs, and a third run was therefore made to establish the cell constants more exactly.

For the calibration run, the wavelength was carefully measured using a specimen of mixed silicon and nickel powders. From the 111 and 200 Ni peaks and the 111, 220 and 311 Si peaks, extrapolating to $\theta = 90°$, the wavelength was determined to be 2·434 (2) Å. With unchanged settings, a 24 h run with a C_2I_4 sample at 4 K was carried out, from $2\theta = 18$ to 99°, followed by a 30-parameter refinement which yielded the values shown in Table 3. The resulting cell constants were then used to calibrate data sets 1 and 2, giving mean calibration factors for the cell constants of 0·98458 (12) and 0·98650 (15) respectively, and effective wavelengths of 1·538 (1) and 2·407 (2) Å. Applying these factors yields the corrected values shown in Tables 3 and 1, from which it can be seen that the agreement between the three sets of cell constants after calibration is very good. Corrected values will be assumed for the remainder of the discussion.

Discussion of results

The refined parameters for all three data sets are shown in Table 3. Going from the 38-parameter to the 30-parameter refinement for data set 2, the residuals decrease slightly and no change in refined parameters is significant at the 0·05 level. Thus, removing the C atoms from the C(2) and C(4) sites improves the quality of fit and does not affect the positions of the remaining atoms, and it is unnecessary to postulate a statistical occupancy of these sites. We can conclude then that both *A* and *B* molecules are completely ordered, with C=C bonds lying approximately along **a***. Fig. 4 shows a projection of the C_2I_4 molecule on the (010) plane. In the remaining discussions only the 30-parameter values will be referred to for data set 2.

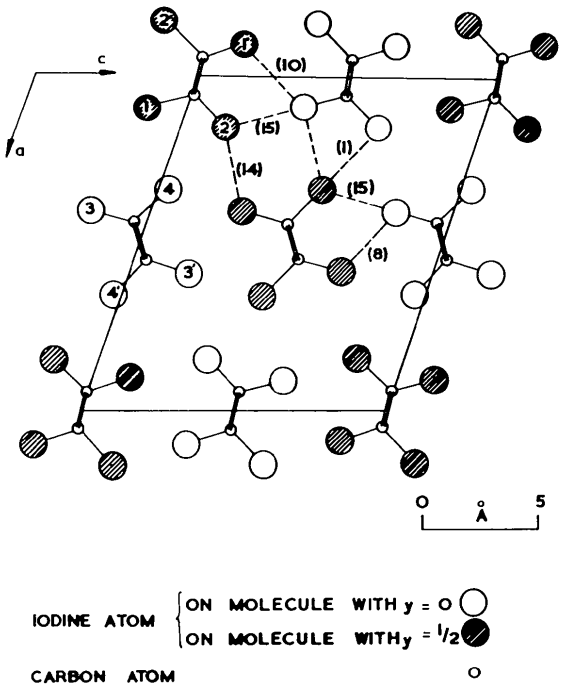

Fig. 4. Projection of the C_2I_4 molecule on the (010) plane. The contact numbers are as specified in Table 1.

Normalization and weighting

The availability of three independent data sets, collected from the same specimen at different wavelengths, permits an analysis of the differences between refined parameters and hence a check on the validity of the estimated standard deviations (e.s.d.'s) claimed for them. Any differences found between data sets for the same refined parameter should be caused only by random variation. They should thus be consistent with having been drawn from a Gaussian distribution with a mean of zero and a standard deviation derived appropriately from the e.s.d.'s claimed for that parameter.

For each parameter, the more precise data set 2 was used as reference and differences calculated by subtracting the set 1 and set 3 values in turn from that for set 2. The corresponding e.s.d.'s were obtained from the sum of the squares of the appropriate e.s.d.'s for the two sets: $\sigma_{a-b} = (\sigma_a^2 + \sigma_b^2)^{1/2}$.

Each difference was expressed in terms of its e.s.d., and hence, by reference to tables for Gaussian distributions (Wilson, 1952), was converted to the nominal probability p that it was obtained by chance variation. To obtain a sufficiently large number of samples, the differences for fractional coordinates were grouped together for each pair of data sets, giving 12 values for data sets 2 and 1, and 18 for sets 2 and 3. For the cell constants, both data set comparisons were combined to give a single group of eight values.

The distributions of probability values for the three groups are given in Table 4, and show that, in this case at least, the e.s.d.'s derived by the Rietveld method are of approximately the right order of magnitude, but have been systematically distorted, being too large for some groups of parameters and too small for others. For example, the agreement between the sets of refined cell constants is considerably better than their claimed e.s.d.'s would suggest: only one difference out of eight achieves a nominal probability $p < 0.5$. This implies that the cell-constant e.s.d.'s have been overestimated. Similarly, it is clear that the e.s.d.'s for fractional coordinates have been considerably underestimated.

An estimate of the normalization factors, required to scale the claimed e.s.d.'s to their true values, can be obtained for each parameter group by comparing the nominal p values with the actual frequency distribution observed. For a standard Gaussian distribution, 50% of samples should exceed 0·674 standard deviations in magnitude, whereas for the cell-constant differences the 50% point is found to be at 0.45σ, so that the claimed e.s.d.'s have been overestimated by a factor of 1·5.

Similarly, for the fractional coordinates, the e.s.d.'s of the differences have been underestimated by factors

Table 4. *Analysis of differences between refined parameters*

Distribution of differences between data sets for groups of refined parameters; p is the probability of an observed difference arising by chance if the claimed e.s.d.'s are correct, assuming sampling from a Gaussian distribution.

Parameter group	Data sets	Group total	Number of differences for which p is: <0.5	<0.1	<0.05	<0.01	<0.001
Cell constants	2–1, 2–3	8	1	0	0	0	0
Fractional	2–1	12	11	10	9	3	2
coordinates	2–3	18	17	5	3	2	1
After normalization							
Fractional	2–1	12	9	1	0	0	0
coordinates	2–3	18	6	1	1	0	0

of 3·7 (set 2 − set 1) and 1·8 (set 2 − set 3) respectively. In order to separate these values into factors for the individual data sets, a further assumption is required. Because of their similar wavelengths, and hence resolutions, it seems reasonable to assign the same normalization factor of approximately 2 to data sets 2 and 3 (*ca* 2·4 Å), in which case a factor of approximately 3 is obtained for set 1 (1·54 Å). After applying these to normalize the claimed e.s.d.'s, the distributions of probabilities for both groups of fractional coordinate differences become entirely satisfactory (see Table 4).

Only a very rough estimate is possible in the case of the C site-occupancy e.s.d.'s, but, on the basis that the structure is ordered, they have been underestimated by a factor of about 10 for data set 1, and are tolerably accurate for data set 2.

Because the e.s.d.'s are neither uniformly too large nor too small, the deficiency must lie in the error-propagation relations that link profile differences with e.s.d.'s for the various classes of parameter. The trend of agreement improving with longer wavelength strongly suggests that the precision of the refined parameters depends on the extent to which individual peaks are resolved (or at least their steeply sloping sides). Thus, for a given instrumental resolution, the relative weight to be allotted to a particular data set refined by the Rietveld method appears to be represented better by λ/σ^2 than by the more usual $1/\sigma^2$, where σ is the mean e.s.d. and λ the wavelength. This expression gives relative weights for data sets 1, 2 and 3 of approximately 2:5:3, which agree well with the absolute variances after normalization and have been used to calculate the weighted mean bond lengths and angles shown in Tables 1 and 2.

Weighted mean results

Weighted mean values for the C_2I_4 structure at 4 K are shown in the final column of Table 1, with e.s.d.'s calculated from the individual absolute e.s.d.'s after normalization. Chemically equivalent intramolecular parameters have been averaged for the *A* and *B* molecules, and can be seen (Table 2) to be in excellent agreement with the vapour-phase electron-diffraction values of Strand (1967). The only discrepant value is that for the C=C bond length, which differs by $2{\cdot}8\sigma$ as a result of the low value obtained for molecule *A*. As the equivalent bond in molecule *B* is in very close agreement with the electron-diffraction value, the discrepancy is almost certainly not a real effect.

By comparison with the X-ray data of Kipps (1973), it is apparent that the unit cell at 4 K has contracted from its dimensions at room temperature by 0·66% along **a**, 2·3% along **b** and 1·4% along **c**, while β has fallen from 109·32 to 108·35°. Combining these data with the room-temperature structural data of Kitaigorodsky *et al.* (1953), it can be seen that this is due mainly to a contraction of 1·5% in the two shortest intermolecular I—I contacts.

The present study appears to have taken the Rietveld profile refinement method fairly close to the limit of what is feasible, at least for neutron data of this resolution (half-width *ca* 0·7° of 2θ). Data set 1 included approximately 900 calculated lines up to $2\theta = 110°$, with up to 50 contributing to a single observed diffraction count. Thermal vibrational parameters were hardest to determine, particularly in the presence of doubtfully extrapolated background estimates. Population parameters were considerably more stable, being nearly as reliable as the fractional coordinates. Cell-constant determinations were very precise, even with the low-resolution 1·54 Å data, and could clearly have tolerated some further loss of data quality. There appear to be substantial advantages to working with more than one independent data set in these circumstances.

Conclusions

The structure of tetraiodoethylene at 4 K has been redetermined by neutron powder diffraction. The lattice parameters have been measured together with interatomic distances, and the heavy-atom structure of Kitaigorodsky *et al.* (1953) confirmed, showing that no major phase transition has occurred. It proved possible to locate the C atoms, and to show that in both molecules the C=C bonds are fully ordered in the solid at 4 K and aligned approximately along **a***, as predicted by Thackeray *et al.* (1974). Because of the high potential-energy barrier to molecular rotation, it is to be expected that the ordering will persist at room temperature.†

We are grateful to Dr A. W. Hewat for making the experimental measurements for data set 1, and to Dr B. T. M. Willis for encouragement and assistance.

† This has been confirmed by a room-temperature structure determination, which will be reported separately.

References

DAHL, T. & HASSEL, O. (1965). *Acta Chem. Scand.* **19**, 2000–2001.

DAHL, T. & HASSEL, O. (1968). *Acta Chem. Scand.* **22**, 715–716.

HEWAT, A. W. (1973). Fortran IV version of the Rietveld computer program, modified for anisotropic thermal vibrations. AERE Harwell.

KHOTSYANOVA, T. L., KITAIGORODSKY, A. I. & STRUCHKOV, YU. T. (1952). *Dokl. Akad. Nauk. SSSR*, **85**, 785–788.

KHOTSYANOVA, T. L., KITAIGORODSKY, A. I. & STRUCHKOV, YU. T. (1953). *Zh. Fiz. Khim. SSSR*, **27**, 1330–1343.
KIPPS, M. (1973). MSc Dissertation, Univ. of Surrey.
KITAIGORODSKY, A. I. (1961). *Organic Chemical Crystallography*, pp. 165–168, 252–253, London: Heywood.
KITAIGORODSKY, A. I., KHOTSYANOVA, T. L. & STRUCHKOV, YU. T. (1953). *Zh. Fiz. Khim. SSSR*, **27**, 1490–1502.
RIETVELD, H. M. (1969*a*). Reactor Centrum Nederland, Res. Rep. RCN-104.
RIETVELD, H. M. (1969*b*). *J. Appl. Cryst.* **2**, 65–71.
STRAND, T. G. (1967). *Acta Chem. Scand.* **21**, 2111–2118.
THACKERAY, D. P. C., SHIRLEY, R., ORALRATMANEE, C., KIPPS, M. & STACE, B. C. (1974). *J. Mol. Struct.* **20**, 293–299.
WILSON, E. B. (1952). *An Introduction to Scientific Research*, p. 237. New York: McGraw-Hill.

Acta Cryst. (1977). B**33**, 1773–1780

Structural Phase Transition in Polyphenyls. IV. Double-Well Potential in the Disordered Phase of *p*-Terphenyl from Neutron (200 K) and X-ray (Room-Temperature) Diffraction data

PAR J. L. BAUDOUR AND H. CAILLEAU

Département de Physique Cristalline et Chimie Structurale, ERA au CNRS n° 015, Université de Rennes, avenue du Général Leclerc, 35031 Rennes Cédex, France

AND W. B. YELON*

Institut Max von Laue–Paul Langevin, PB 156, 38042 Grenoble Cédex, France

(*Received* 15 *October* 1976; *accepted* 15 *November* 1976)

New neutron-diffraction data collected at 200 K with deuterated *p*-terphenyl, and published X-ray data collected at room temperature with protonated *p*-terphenyl, have been used to determine the characteristics of the double-well potential for the librations of the central ring about the long molecular axis, in the disordered phase. A picture of the double well is obtained simply by halving the atoms outside the molecular axis and imposing constraints on their geometries and thermal parameters. The *R* values compared with that obtained with the simple-well model, are significantly improved. The deuterated benzene rings, compared to the protonated ones, show a systematic and hard-to-explain distortion: all the internuclear C—C bond lengths parallel to the long axis are shortened and the others lengthened, the mean bond lengths being the same in the two compounds. The double-well potential-barrier height is found to be about 0·6 kcal mol^{-1} at 200 K and at room temperature. This value is in good agreement with that given by potential-energy calculations. The rotation angle between the two wells is about 26°. Only for the internal *g* mode is the thermal energy kT sufficient to bring the rings near the top of the barrier. For the central-ring librations the doubly peaked distribution function is an argument for an order–disorder regime. However, the smallness of the double-well barrier height suggests that the *p*-terphenyl structural phase transition is near the boundary between the order–disorder and displacive regimes.

Introduction

The structure of *p*-terphenyl in the low-temperature ordered phase has recently been solved (Baudour, Delugeard & Cailleau, 1976). The ordering results from the stabilization of the central ring of each molecule in one of the two bottoms of a double-well potential, at an average angle of 16° from the mean planar configuration seen by diffraction at room temperature. The external rings are stabilized at about 5° from the mean configuration, but in the opposite sense of the central rings. The conformations of the four independent nonplanar molecules in the unit cell, given by X-ray diffraction at 110 K (space group $P\bar{1}$), have been confirmed by recent potential energy calculations (Ramdas & Thomas, 1976).

Phase transitions are often referred to as either the displacive or order–disorder type. The borderline between the two types is not sharp, however, as they

* Present address: University of Missouri Research Reactor COLUMBIA, Missouri 65201, USA.